

Source Apportionment of Elemental Carbon in Beijing, China: Insights from Radiocarbon and Organic Marker Measurements

Yan-Lin Zhang,^{*,†,‡,§} Jürgen Schnelle-Kreis,^{||} Gülçin Abbaszade,^{||} Ralf Zimmermann,^{||,⊥} Peter Zotter,^{‡,||} Rong-rong Shen,[#] Klaus Schäfer,[#] Longyi Shao,[∇] André S.H. Prévôt,[‡] and Sönke Szidat[†]

[†]Department of Chemistry and Biochemistry & Oeschger Centre for Climate Change Research, University of Bern, 3012 Berne, Switzerland

[‡]Paul Scherrer Institute (PSI), 5232 Villigen-PSI, Switzerland

[§]Yale-NUIST Center on Atmospheric Environment, Nanjing University of Information Science and Technology, Nanjing 210044, China

^{||}Joint Mass Spectrometry Center, Cooperation Group Comprehensive Molecular Analytics, Helmholtz Zentrum München, 85764 Neuherberg, Germany

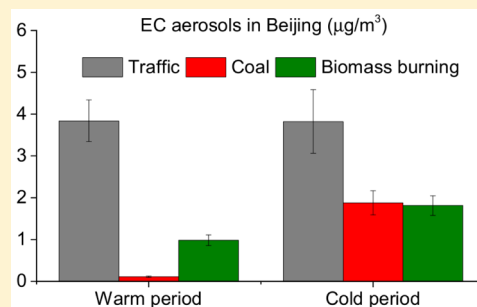
[⊥]Joint Mass Spectrometry Centre, Chair of Analytical Chemistry, Institute of Chemistry University of Rostock, 18059 Rostock, Germany

[#]Institute of Meteorology and Climate Research (IMK-IFU), Karlsruhe Institute of Technology (KIT), 82467 Garmisch-Partenkirchen, Germany

[∇]State Key Laboratory of Coal Resources and Safe Mining, School of Geoscience and Surveying Engineering, China University of Mining and Technology (Beijing), Beijing 100083, China

S Supporting Information

ABSTRACT: Elemental carbon (EC) or black carbon (BC) in the atmosphere has a strong influence on both climate and human health. In this study, radiocarbon (¹⁴C) based source apportionment is used to distinguish between fossil fuel and biomass burning sources of EC isolated from aerosol filter samples collected in Beijing from June 2010 to May 2011. The ¹⁴C results demonstrate that EC is consistently dominated by fossil-fuel combustion throughout the whole year with a mean contribution of 79% ± 6% (ranging from 70% to 91%), though EC has a higher mean and peak concentrations in the cold season. The seasonal molecular pattern of hopanes (i.e., a class of organic markers mainly emitted during the combustion of different fossil fuels) indicates that traffic-related emissions are the most important fossil source in the warm period and coal combustion emissions are significantly increased in the cold season. By combining ¹⁴C based source apportionment results and picene (i.e., an organic marker for coal emissions) concentrations, relative contributions from coal (mainly from residential bituminous coal) and vehicle to EC in the cold period were estimated as 25 ± 4% and 50 ± 7%, respectively, whereas the coal combustion contribution was negligible or very small in the warm period.



1. INTRODUCTION

Atmospheric aerosols adversely affect human health by causing respiratory and cardiopulmonary diseases associated with increased morbidity and mortality.^{1,2} Carbonaceous components are a major fraction of atmospheric aerosols and are often classified into the subfractions organic carbon (OC) and elemental carbon (EC) or black carbon (BC).³ In this study, BC is used as a qualitative and descriptive term not referring to measurement results of any specific properties, whereas BC mass quantified by thermal-optical methods is specified as EC.⁴ As the major light-absorbing part of carbonaceous material, BC exhibits the second largest anthropogenic radiative forcing after carbon dioxide (CO₂).⁵ Recently, it was estimated that 640–4900 premature human deaths could be prevented annually by

utilizing available mitigation measures to reduce BC in the atmosphere.⁶ Due to a relatively short lifetime (~days) in atmosphere, reducing BC emissions may rapidly improve both climate and human health.^{7,8} Therefore, the identification and quantification of different BC sources and their emission source strengths is crucial for the implementation of effective mitigation strategies.

The emission sources of BC are exclusively combustion processes of fossil and nonfossil fuels, although the relative

Received: April 17, 2015

Revised: June 23, 2015

Accepted: June 26, 2015

Published: June 26, 2015

contribution of these two sources still remains uncertain. In recent years, the radiocarbon (^{14}C) measurement of EC has been proven to be a powerful tool for the differentiation between modern (i.e., biomass burning) and fossil (i.e., traffic and coal) sources. ^{14}C is completely depleted in fossil fuel emissions due to its half-life (i.e., 5730 years), whereas ^{14}C in nonfossil carbonaceous materials contains a similar composition as atmospheric CO_2 .^{9,10} Therefore, ^{14}C measurement of the EC fraction directly enables the quantification of its biomass-burning and fossil sources.¹¹ However, the ^{14}C measurement of EC still remains challenging in comparison to total carbon (TC) due to its complex properties¹² and since a clear physical separation between OC and EC is necessary to avoid artifacts in the ^{14}C signal. Nevertheless, recent developments and method adaptations from different groups show more consistent approaches and yield more robust ^{14}C results.^{13,14}

Beijing, the capital of China with about 19.6 million inhabitants in 2010, is one of the largest cities in the world and has become a heavily polluted area due to rapid urbanization and industrialization over the past two decades.¹⁵ In the past decade, many studies have reported the chemical composition and sources of aerosols in Beijing.^{16–23} Most of these studies have focused on source apportionment of organic aerosols (organic matter, OM or OC) by positive matrix factorization (PMF)²⁴ and chemical mass balance (CMB) models²¹ from off-line organic markers measurement or online aerosol mass spectrometer measurement. However, only a few studies have reported year-round source apportionment results of BC. For example, Duan et al. (2004) demonstrated biomass burning and traffic and/or industry emissions are the major sources of both OC and EC during summer, while coal combustion is the dominant contributor during the winter heating period, although quantification of contributions from each source still remains uncertain. Based on PMF model analysis, about 50% of OC and EC in Beijing were associated with biomass-burning processes.²⁵ In contrast, most recent source-diagnostic ^{14}C studies suggested ~80% contribution from fossil fuels in winter for EC in China.^{15,23,26} A quantitative understanding of the temporal variations and source apportionment of EC in Beijing is still missing and thus crucially necessary. In this study, we determine fossil and biomass-burning contributions to year-round EC aerosols in Beijing by measuring ^{14}C of EC and organic markers for fossil emissions (i.e., hopanes and picene).

2. EXPERIMENTAL SECTION

2.1. Sampling. Twenty four hour integrated $\text{PM}_{4.0}$ samples ($n = 155$) were collected at the ground level on prebaked ($650\text{ }^\circ\text{C}$, 4 h) quartz-fiber filters (diameter: 150 mm) using a high-volume sampler (Digital DHA-80, Switzerland) at a flow rate of ~167 l/min during June 2010 to May 2011 at the campus of the China University of Geosciences, a residential area in North West of Beijing. It should be noted that during the whole campaign the actual sampling flow of ambient air was 167 instead of 500 L/min as a default setting due to an airflow shortcut from the interior of the sampler. As a consequence to the changed flow volume, the cut off of the sampler (original setting: $2.5\text{ }\mu\text{m}$) had to be recalculated following the impactor design theory.^{27–29} It was found that particles smaller than $4\text{ }\mu\text{m}$ (i.e., $\text{PM}_{4.0}$) were collected onto the filters. However, a comparison of ^{14}C results obtained from the current study was not significantly different from those found for $\text{PM}_{2.5}$ samples during winter 2013 (see Supporting Information (SI), Figure S1).²³ Our previous work has also shown that there is no significant difference of EC source

signatures (fossil vs nonfossil) between $\text{PM}_{1.0}$, $\text{PM}_{2.5}$, and $\text{PM}_{10.0}$ at other locations (SI Table S1).³⁰ Further, since EC almost exclusively derives from combustion sources, the size of EC particles from China's source samples is mostly smaller than $1\text{ }\mu\text{m}$ ^{31,32} and the majority of EC mass (~80%) in urban site of China resides in particles smaller than $3.2\text{ }\mu\text{m}$ in diameter and the fine mode peaks at around either 0.42 or $0.75\text{ }\mu\text{m}$.³³ As a result, the cut size present in our study generally would not affect the results of relative fossil and nonfossil contribution of EC of aerosols because EC is dominated in the fine particles. After sampling, filters were wrapped in aluminum foil and stored in a freezer at $-20\text{ }^\circ\text{C}$ before analysis. Every second week, one field blank was collected.

2.2. Elemental Carbon Measurement. A filter cut of 1.5 cm^2 was used for EC measurement. The EC concentrations were measured using a thermo-optical OC/EC analyzer (model 4L, Sunset Laboratory Inc.), equipped with a nondispersive infrared (NDIR) detector following the thermal-optical transmittance protocol (TOT) EUSAAR2.³⁴ A high uncertainty of 20% is considered for all measured EC concentrations to account for possible differences between different TOT protocols.^{35,36} It should be noted that only the absolute EC concentration is affected by this additional uncertainty, whereas the relative fossil and nonfossil contribution is only influenced by the combined uncertainty of the ^{14}C measurement of EC and the bomb peak correction, which is on average 5% (see below). No EC was detected on blank filters and consequently no blank correction was necessary.

2.3. Radiocarbon (^{14}C) Measurement of EC. A filter cut of $1\text{--}6\text{ cm}^2$ (corresponding to $5\text{--}30\text{ }\mu\text{gC}$) was used for ^{14}C analysis. The Swiss_4S protocol was applied for the EC isolation for the ^{14}C analysis using a Sunset OC/EC analyzer connected to a gas preparation line as described by.¹⁴ This special protocol is optimized to minimize the bias in the ^{14}C result of EC from OC charring or losses of the least refractory EC during the OC removal. In brief, to minimize positive artifacts from OC charring, water-soluble OC is first eliminated by a water-extraction pretreatment and the remaining water-insoluble OC is then removed using the Sunset OC/EC analyzer with a thermal treatment in three steps: (1) $375\text{ }^\circ\text{C}$ for 150 s in pure oxygen (O_2); (2) $475\text{ }^\circ\text{C}$ for 180 s in O_2 ; (3) $450\text{ }^\circ\text{C}$ for 180 s followed by 180 s at $650\text{ }^\circ\text{C}$ in helium. Finally, in step four EC is isolated by the combustion of the remaining carbonaceous material at $760\text{ }^\circ\text{C}$ for 150 s in O_2 . EC recovery is estimated by the ratio $\text{ATN}_t/\text{ATN}_0$, where ATN_0 is the initial attenuation (ATN, see SI), which is related to the total amount of EC on the filter, and ATN_t is the attenuation at the time t , when the EC step (i.e., step 4) begins. By using the Swiss_4S protocol, OC charring is minimized to $4 \pm 3\%$ compared to EC (see SI), which may lead a negligible overestimation of nonfossil EC by less than 3%. This assures the accuracy of ^{14}C measurement in EC. The EC recovery in this study was estimated as $85 \pm 5\%$, thus presenting almost the entire continuum of EC. ^{14}C results in EC were extrapolated to 100% EC recovery ($f_{\text{M,EC,corrected}} = \text{slope} \times (1 - \text{EC recovery}) + f_{\text{M,EC}}$) to account for the less refractory EC, mainly from wood burning, which is removed during steps 1–3.¹⁴ The slope of 0.31 is deduced from linear regression of the EC recovery and $f_{\text{M,EC}}$.¹⁴ The uncertainty of the reported $f_{\text{M,EC}}$ is obtained by an error propagation of all possible uncertainties including an assigned uncertainty of 10% for the slope, the measurement uncertainty of $f_{\text{M,EC}}$ (2%) and an assigned uncertainty of 10% for the EC yield, which results to a total average uncertainty of 4%.

The evolving CO₂ in step 4 was separated from interfering gaseous products, cryo-trapped and sealed in glass ampules for ¹⁴C measurements. ¹⁴C measurements of the CO₂ was carried out with the mini radio carbon dating system, MICADAS³⁷ using a gas ion source.³⁸ The ¹⁴C results are presented as fraction of modern (f_M) denoting the ¹⁴C/¹²C content of the sample related to that of the reference year 1950.³⁹ Oxalic acid (HOxII) reference material ($f_M = 1.3407$) and of ¹⁴C-free materials ($f_M = 0$) are used for normalization background correction. The f_M values were further corrected for $\delta^{13}C$ fractionation and for ¹⁴C decay between 1950 and the year of measurement.⁴⁰ The f_M measurement uncertainty for the EC samples is $\sim 2\%$.

2.4. Organic Marker (Hopanes and Picene) Measurements. A filter cut of 1–6 cm² was used for organic marker's measurement. The organic markers picene and hopanes (see Table 2) were quantified using in situ derivatization thermal desorption gas-chromatography time-of-flight mass spectrometry (IDTD-GC-MS, Orasche et al.⁴¹). Briefly, the filter punches were placed into glass liners suitable for an automated thermal desorption unit. Isotope-labeled standard compounds were spiked directly onto the filter surface to account for influences of the matrix for later quantification. Derivatization was performed on the filter by adding of liquid derivatization reagent *N*-methyl-*N*-trimethylsilyl-tri fluoroacetamide (MSTFA, Macherey-Nagel, Germany). During 16 min of desorption time, in addition an in situ derivatization with gaseous MSTFA was carried out. Desorbed molecules were trapped on a precolumn before separation by gas chromatography (BPX-5 capillary column, SGE, Australia). The detection and quantification of compounds was carried out on a Pegasus III time-of-flight mass spectrometer (TOF) using the ChromaTOF software package (LECO, St. Joseph, MI). The blank values of hopanes and picene were below the detection limit (0.02 ng/m³).

3. RESULTS AND DISCUSSIONS

3.1. Temporal Variation of EC. Figure 1 shows EC concentrations during the whole sampling period. EC concen-

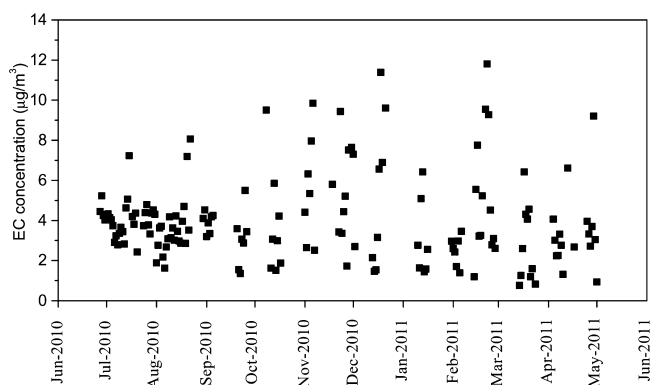


Figure 1. Temporal variation of EC concentrations ($\mu\text{g}/\text{m}^3$, $n = 155$) in Beijing, China.

trations range from 0.8 to 11.8 $\mu\text{g}/\text{m}^3$, and the average of $4.0 \pm 2.2 \mu\text{g}/\text{m}^3$ is within the range (2.3–7.4 $\mu\text{g}/\text{m}^3$) reported by previous studies for Beijing.^{21,42} The EC concentrations are significantly lower (t test with $p < 0.05$) during the warm period (i.e., average from March to October is $3.6 \pm 1.5 \mu\text{g}/\text{m}^3$) than in the cold period (i.e., average from November to February is $4.8 \pm 2.9 \mu\text{g}/\text{m}^3$). It should be noted that the frequency of samples with EC larger than 4.5 $\mu\text{g}/\text{m}^3$ in the cold period is much larger than

that in the warm period, indicating a higher primary particulate pollution from enhanced anthropogenic emissions during the cold period. A similar seasonal trend was also observed by ref 43. This seasonality is likely attributed to increased emissions from residential heating using coal or biofuel. The lower EC abundance in the warm period is mainly caused by reduced heating-related coal/biofuel emissions on the one hand and a higher mixing layer on the other hand. It should be pointed out that EC concentration in summer at the studied site is still higher than those observed in many other cities during summer such as Barcelona, Spain (1.2 $\mu\text{g}/\text{m}^3$),⁴⁴ Paris, France (1.4 $\mu\text{g}/\text{m}^3$)⁴⁵ or Pittsburgh, PA (0.89 $\mu\text{g}/\text{m}^3$).⁴⁶

3.2. ¹⁴C Results of EC: Fraction of Modern. In order to further investigate the sources of EC, 14 samples from different seasons were selected for the analysis of ¹⁴C of the EC fraction (Table 1). In order to address the air quality problems of Beijing,¹⁵ we characterized EC sources for days with medium and heavy air pollution during the warm and cold periods. Therefore, samples were selected for radiocarbon analysis with EC concentrations $> 3 \mu\text{g}/\text{m}^3$, which includes about $2/3$ of all daily samples shown in Figure 1, representing $\sim 82\%$ of the integrated EC burden of all samples. However, EC sources of background days are not considered. The values for $f_M(\text{EC})$ ranged from 0.10 to 0.34 with a mean of 0.23 ± 0.06 , indicating a dominance of fossil sources of EC in Beijing throughout the year. Since EC is only emitted as primary aerosol by combustion from either biomass or fossil fuels (i.e., coal and vehicle emissions), $f_M(\text{EC})$ particularly tracks the change of EC sources. The lowest $f_M(\text{EC})$ is found in summer (0.15), indicating the importance of vehicle emissions since the coal consumption is much reduced compared to other seasons. $f_M(\text{EC})$ is higher by 60% in the rest of the year than in summer, suggesting that EC from biomass burning becomes substantial during the other seasons. Further discussions of source apportionment of fossil EC will be presented in Section 3.4.

3.3. Fossil vs Biomass Burning EC. The fraction of modern (f_M) is not identical to the fraction of nonfossil (f_{NF}) due to increased ¹⁴C content of the atmosphere from the nuclear bomb test in the 1950s and 1960s. A reference value representing the modern ¹⁴C content of biomass burning aerosols ($f_{\text{M,bb}}$) during the sampling period compared to 1950 before the bomb test is used to convert f_M to f_{NF} :

$$f_{\text{NF}}(\text{EC}) = f_M(\text{EC})/f_{\text{M,bb}} \quad (1)$$

The value of $f_{\text{M,bb}}$ is estimated as 1.12 ± 0.05 .⁴⁷ Since biomass burning (including biofuel combustion) is the only source of nonfossil EC, the fraction of nonfossil (f_{NF}) equals to the fraction of biomass burning (f_{BB}). The fraction of fossil fuels (f_{FF}) is determined by

$$f_{\text{FF}} = 1 - f_{\text{BB}} \quad (2)$$

Fossil-fuel and biomass-burning EC concentrations (i.e., EC_{FF} and EC_{BB} , respectively) are calculated as follows:

$$\text{EC}_{\text{FF}} = \text{EC} \times (1 - f_{\text{BB}}) \quad (3)$$

$$\text{EC}_{\text{BB}} = \text{EC} \times f_{\text{BB}} \quad (4)$$

Figure 2 shows the source apportionment results of EC. The EC_{FF} concentrations range from 2.5 to 7.5 $\mu\text{g}/\text{m}^3$, whereas the corresponding range for EC from biomass burning (EC_{BB}) was 0.4–2.4 $\mu\text{g}/\text{m}^3$. EC_{FF} values are on average 4.6 times higher than EC_{BB} , corresponding to a mean contribution of EC_{FF} to total EC

Table 1. Sampling Dates and Temperature (T) of the Selected Aerosol Samples for ^{14}C Measurements and Their Corresponding EC Concentration, Fraction of Modern (f_M), Fraction of Biomass Burning (f_{BB}), Fraction of Fossil-Fuel (f_{FF}), Biomass-Burning EC (EC_{BB}) and Fossil-Fuel EC Concentrations (EC_{FF})

date	T °C	EC ($\mu\text{g}/\text{m}^3$)	f_M	f_{BB}	f_{FF}	EC_{BB} ($\mu\text{g}/\text{m}^3$)	EC_{FF} ($\mu\text{g}/\text{m}^3$)
7/3/2010	30	4.30	0.15 ± 0.02	0.14 ± 0.02	0.86 ± 0.02	0.59 ± 0.07	3.7 ± 0.46
7/5/2010	32	3.88	0.10 ± 0.01	0.09 ± 0.01	0.91 ± 0.01	0.35 ± 0.05	3.53 ± 0.55
7/25/2010	30	4.38	0.18 ± 0.01	0.17 ± 0.01	0.83 ± 0.01	0.73 ± 0.06	3.65 ± 0.29
7/27/2010	31	3.90	0.19 ± 0.01	0.18 ± 0.01	0.82 ± 0.01	0.69 ± 0.05	3.21 ± 0.25
10/8/2010	17	9.50	0.25 ± 0.02	0.23 ± 0.02	0.77 ± 0.02	2.19 ± 0.21	7.31 ± 0.7
11/28/2010	-1	7.30	0.34 ± 0.02	0.31 ± 0.02	0.69 ± 0.02	2.26 ± 0.15	5.04 ± 0.33
11/30/2010	-1	7.64	0.28 ± 0.02	0.25 ± 0.02	0.75 ± 0.02	1.95 ± 0.13	5.7 ± 0.39
2/15/2011	-6	5.55	0.25 ± 0.02	0.23 ± 0.02	0.77 ± 0.02	1.27 ± 0.09	4.28 ± 0.31
2/16/2011	-3	7.75	0.25 ± 0.02	0.23 ± 0.02	0.77 ± 0.02	1.77 ± 0.13	5.98 ± 0.45
2/21/2011	1	9.34	0.21 ± 0.01	0.19 ± 0.01	0.81 ± 0.01	1.82 ± 0.14	7.52 ± 0.57
3/18/2011	8	4.27	0.23 ± 0.02	0.21 ± 0.02	0.79 ± 0.02	0.91 ± 0.08	3.36 ± 0.29
3/20/2011	7	4.50	0.30 ± 0.02	0.27 ± 0.02	0.73 ± 0.02	1.23 ± 0.09	3.27 ± 0.23
4/13/2011	17	6.61	0.26 ± 0.02	0.24 ± 0.02	0.76 ± 0.02	1.59 ± 0.13	5.02 ± 0.4
4/30/2011	16	3.06	0.21 ± 0.02	0.19 ± 0.02	0.81 ± 0.02	0.58 ± 0.06	2.48 ± 0.27

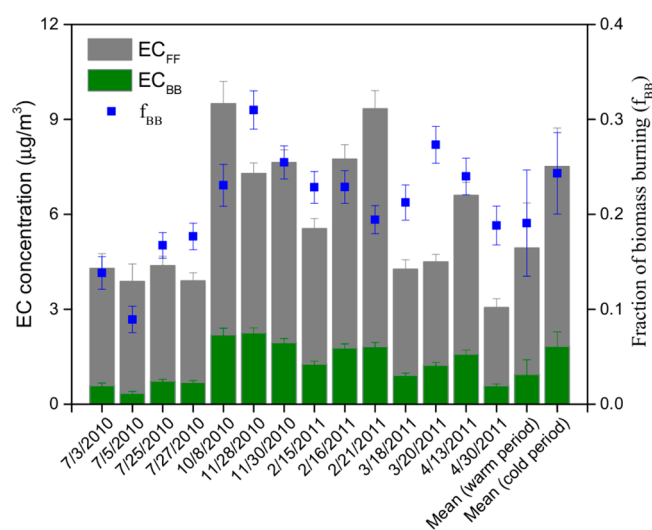


Figure 2. Mass concentrations ($\mu\text{g}/\text{m}^3$) of EC from biomass burning and fossil-fuel combustion (EC_{BB} and EC_{FF} , respectively) as well as fractions of biomass-burning EC to total EC (f_{BB}) in Beijing with 1σ uncertainties.

of $79\% \pm 6\%$ (ranging from 70% to 91%). The measured fossil contributions to EC are comparable to those previously reported with a similar ^{14}C -based approach in Beijing during winter 2011⁴⁸ and winter 2013,²³ but are higher than for an urban site in Guangzhou, China (winter 2012/2013: $71 \pm 10\%$)⁴⁹ and a background site on the Hainan Island, South China (annual average 2005/2006: 25–56%)⁴⁷ as well as 16 urban and rural sites across Switzerland (winter 2007/2008–2011/2012: 13–88%).¹¹ Higher EC_{FF} concentrations were observed in the cold period, most probably associated with larger coal combustion for heating. However, relative contributions from fossil combustion are even lower in the cold season than in the warm season, implying that biomass-burning emissions are also considerably important for the EC increment in the cold season. It should be noted that it is common practice to burn maize and wheat residues especially in the rural areas without central space heating and gas supplying systems and a large fraction of this biomass burning is emitted as OC and EC.⁵⁰ The contribution of these biomass-burning emissions to EC in cold seasons is likely very important due to lower combustion efficiency for residential

biomass burning than for coal boilers. By subtracting mean values of EC_{BB} and EC_{FF} in the warm period from those in the cold period, the excess is estimated as $0.82 \pm 0.40 \mu\text{g}/\text{m}^3$ and $1.75 \pm 0.52 \mu\text{g}/\text{m}^3$ for EC_{BB} and EC_{FF} , respectively. Biomass burning accounted for on the average 32% of the excess during the cold period, which is significantly higher than the contribution of EC_{BB} (19%) during the warm period, but lower than estimations from PMF model analysis (50%).²⁵

3.4. Fossil EC from Coal Combustion and Vehicle Emissions. Hopanes are abundant in crude oils, coal and lubricants.⁵¹ They have been identified in emissions from heating oil burning,⁵² coal burning⁵³ and vehicles.⁵⁴ Table 2 presents hopane concentrations in the warm and cold periods and the difference between these two seasons. As shown in Figure 3 and Table 2, the total identified hopanes mass concentrations show a clearly seasonal trend with maximum in the cold period ($68.6 \pm 28.7 \text{ ng}/\text{m}^3$) and minimum in the warm period ($17.9 \pm 6.5 \text{ ng}/\text{m}^3$). The hopane molecular patterns differ substantially with the type of the fossil source, and therefore potentially allow a distinction of coal combustion and vehicle emissions.^{55,56} For example, the ab-hopane/(ab-hopane+ba-hopanes) ratio (i.e., 30ab/(30ab+30ba)) increases with increasing diagenesis and catagenesis of the sediments. This ratio, also called hopane index, is >0.9 in crude oil⁵⁷ and 0.1–0.6 in different types of coal.^{53,58} In typical petroleum, the R/S-epimerization at C22 has an equilibrium S/(S+R) ratio, the so-called homohopane index (i.e., 31abs/31abs+31abR) of ~ 0.6 ,⁵⁹ whereas this ratio ranges from about 0.1 for lignite coal to ~ 0.4 for bituminous coal. As seen in Table 2, both the hopane index (0.84 ± 0.11) and the homohopane index (0.56 ± 0.04) in the warm period are very close to those in vehicle exhausts, suggesting that contribution of coal burning was negligible or very small in summer in Beijing. In contrast, both ratios found in the cold period (0.57 ± 0.06 and 0.46 ± 0.07 for hopane index and the homohopane index, respectively) are between those of petroleum and coal-burning emissions, indicating additional fossil-fuel emissions from solid coal combustion. Moreover, picene (a specific marker of coal combustion) was also determined in our study (Figure 3 and Table 2) and considerable concentrations are observed during the cold period (i.e., ranging from 0.34 to $4.48 \text{ ng}/\text{m}^3$ with a mean of $1.82 \pm 0.99 \text{ ng}/\text{m}^3$), in contrast to the warm period, when concentrations were often below the detection limit or very small. If we assume that meteorological factors (i.e., wind speed

Table 2. Range and Mean (\pm Standard Deviation) Concentrations of Hopanes (ng/m^3), Picene (ng/m^3), Total EC ($\mu\text{g}/\text{m}^3$), Fossil-Fuel EC (EC_{FF}) ($\mu\text{g}/\text{m}^3$) and Picene-to- EC_{FF} Emission Ratio ($\text{ng}/\mu\text{g}$) in the Warm and Cold Periods and the Excess in the Cold Period

substance	abbreviation	warm period ($n = 22$)		cold period ($n = 15$)		excess	
		range	mean	range	mean	mass	%
18 α (H)-22,29,30-trisnorhopane	Ts	0.39–3.80	1.52 \pm 1.18	0.93–3.69	2.21 \pm 0.85	0.69	46
17 α (H)-22,29,30-trisnorhopane	Tm	0.58–2.68	1.12 \pm 0.49	2.13–13.14	7.58 \pm 3.38	6.46	577
17 α (H),21 β (H)-30-norhopane	29ab	0.87–6.01	3.68 \pm 1.45	4.92–33.66	16.13 \pm 7.61	12.45	339
17 β (H),21 α (H)-30-norhopane+17 α (H),21 α (H)-30-norhopane	29ba	0.33–2.84	1.27 \pm 0.77	1.68–16.31	10.41 \pm 4.75	9.13	718
17 α (H),21 β (H)-30-hopane	30ab	1.33–6.68	4.14 \pm 1.53	3.03–20.64	12.60 \pm 5.61	8.45	204
17 β (H),21 α (H)-30-hopane	30ba	0.49–2.21	1.02 \pm 0.51	1.7–16.43	9.67 \pm 4.54	8.65	847
17 α (H),21 β (H)-22S-homohopane	31abS	0.69–3.35	1.98 \pm 0.78	1.62–5.14	3.31 \pm 1.16	1.33	67
17 α (H),21 β (H)-22R-homohopane	31abR	0.5–2.28	1.54 \pm 0.50	0.95–7.49	3.99 \pm 1.63	2.45	159
17 α (H),21 β (H)-22S-bishomohopane	32abS	0.63–2.45	1.52 \pm 0.48	0.94–4.43	2.89 \pm 1.02	1.37	90
17 α (H),21 β (H)-22R-bishomohopane	32abR	0.35–4.30	1.46 \pm 0.92	0.83–3.81	2.48 \pm 0.91	1.03	70
Subtotal		2.49–24.36	17.88 \pm 6.45	17.79–120.98	68.63 \pm 28.7	50.75	284
hopane index: 30ab/(30ab+30ba)		0.61–1	0.84 \pm 0.11	0.49–0.66	0.57 \pm 0.06	0.49 ^a	
homohopane index: 31abS/(31abS+31abR)		0.46–0.63	0.56 \pm 0.04	0.38–0.63	0.46 \pm 0.07	0.35 ^a	
picene		0–0.17	0.02 \pm 0.05	0.34–4.48	1.82 \pm 0.99	1.79	7576
EC ^b		3.1–9.5	4.9 \pm 2.0	5.6–9.3	7.5 \pm 1.4	2.6	52
EC _{FF} ^b		2.5–7.3	3.9 \pm 1.4	4.3–7.5	5.7 \pm 1.2	1.8	43
(picene/EC _{FF}) ^b		0–0.09	0.02 \pm 0.03	0.24–0.41	0.34 \pm 0.07	1.0 ^a	

^aThese ratios are determined from the masses of the individual components for the excess in the cold period. ^bThe values are obtained from a subset of samples, which are measured for radiocarbon ($n = 9$ and 5 for the warm and cold periods, respectively).

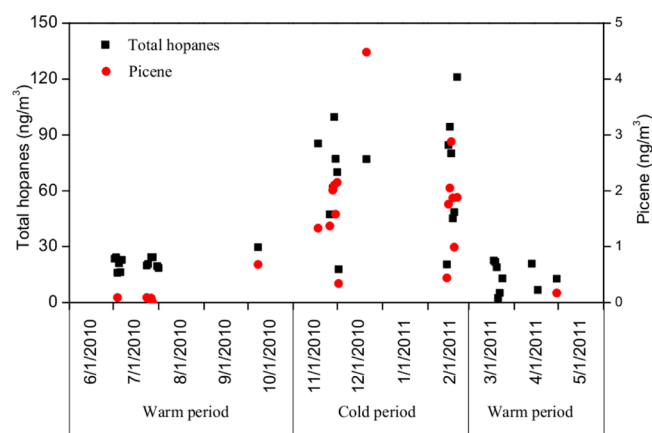


Figure 3. Temporal variation ($n = 35$) of total identified hopanes (see in Table 2) and picene concentrations (ng/m^3) in Beijing, China. The interval of x -axis is 30 days.

and boundary layer height) equally affected both the EC_{FF} and picene concentrations then the difference between the cold and the warm periods for EC_{FF} and picene (i.e., $\Delta\text{EC}_{\text{FF}}$ and Δpicene , respectively) can be attributed only to additional coal combustion. This assumption is also supported by a recent study, in which primary organic aerosols from traffic-related emissions were only found to be $\sim 10\%$, which was even smaller for high pollution events than for low pollution events in winter Beijing.¹⁵ The emission ratio picene/EC for coal combustion is therefore estimated as 1.1 ($\text{ng}/\mu\text{g}$) by

$$(\text{picene}/\text{EC})_{\text{coal}} = \Delta\text{picene}/\Delta\text{EC}_{\text{FF}} \quad (5)$$

The uncertainty of $(\text{picene}/\text{EC})_{\text{coal}}$ is estimated to be 0.22 by an error propagation of possible uncertainties including by assigning 10% as the uncertainty of Δpicene and 20% as the uncertainty of $\Delta\text{EC}_{\text{FF}}$ associated with a overestimation of the EC_{coal} or $\text{EC}_{\text{traffic}}$ in winter.

It should be pointed out that picene may not be stable in summer,⁶⁰ however, the emission ratio estimated by our approach would only change by $<3\%$ if assuming 0–50% of picene in summer has decayed through photochemical transformations. This emission ratio is comparable to the calculated emission ratios for Chinese residential bituminous coal (0.8) combustion but much lower than those found in residential anthracite (2.7), and coal briquette (3.2) combustion.⁶¹ Similarly, the hopane and homohopane indexes for the excess between the cold and warm period is estimated as 0.49 and 0.35 (Table 2), respectively, which are very close to those in residential combustion of bituminous coal (0.52 and 0.37 for the hopane and homohopane indexes, respectively), but very different from typical emission ratios in mineral-oil-based sources (i.e., fuel oil consumption and vehicular emissions) (i.e., hopane index >0.9 and homohopane index in the range of 0.54–0.67).^{53,56,59} This suggests that the bituminite is a dominant contributor of the excess EC, which is associated with the highest EC emission factor from bituminous coals compared to other coal types on one hand and a larger percentage (78%) of bituminous coal in total raw coal in 2000 in China on the other hand.⁶²

The fraction of traffic and coal combustion to EC particles is further calculated by

$$\text{EC}_{\text{coal}} = \text{picene}/(\text{picene}/\text{EC})_{\text{coal}} \quad (6)$$

$$\text{EC}_{\text{traffic}} = \text{EC}_{\text{FF}} - \text{EC}_{\text{coal}} \quad (7)$$

The “best estimate” and its associated uncertainty are obtained by Latin-hypercube sampling (LHS).²³ This approach is comparable to Monte Carlo simulation which has been reported in many ¹⁴C-based source apportionment studies.^{63–66} The emission ratio of picene/EC for coal combustion or $(\text{picene}/\text{EC})_{\text{coal}}$ may be overestimated by 25% or underestimated by 50%, if the traffic EC in winter is actually lower or higher than that in summer, respectively. Considering the overall uncertainty of

(picene/EC)_{coal}, a range from 0.75 to 1.5 with a central value of 1.0 is used as the input. The LHS simulation is conducted by generating 3000 random sets of variables. Simulations producing negative solutions are excluded and the median value from the remaining simulations is used as the best estimate, and the 10th and 90th percentiles of the solutions are used as uncertainties.²³

As shown in Figure 4, EC is divided into three major sources: EC_{BB}, EC_{traffic}, and EC_{coal}. The changes in the source pattern

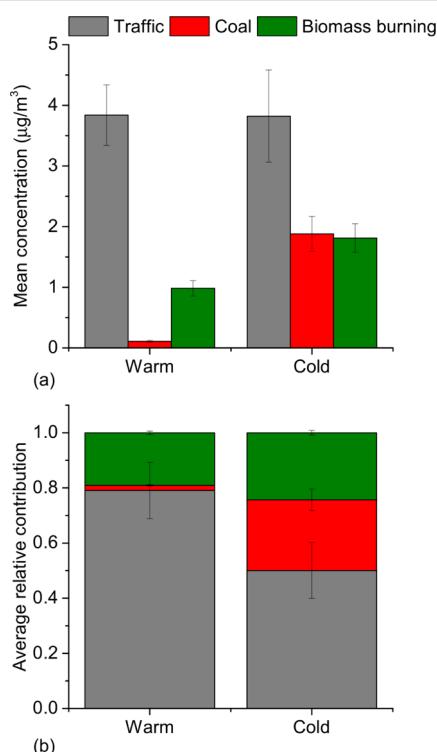


Figure 4. Average EC concentrations (a) and relative contributions (b) from traffic-related, coal and biomass-burning emissions in the warm (March to October) and cold (November to February) periods. Uncertainty bars represent 10th and 90th percentiles from LHS calculations. The integrated probability distribution and sensitivity test (with a variation of ((picene/EC)_{coal})) from the LHS simulation is shown in the Figure S3 and S4 (see SI).

between the warm and cold season are substantial, though vehicle emissions are the most important source of EC in both the warm and cold periods with a mean contribution of $79 \pm 6\%$ and $50 \pm 7\%$, respectively. However, the biomass-burning contribution slightly increased (from 19% to 24%) and the coal combustion contribution increased dramatically in the cold period. The excess of EC between the cold and warm seasons was shared by coal ($68 \pm 4\%$) and biomass burning combustion ($32 \pm 4\%$) sources. The importance of coal contribution in the cold period is also evident by the occurrence of picene and hopanes indices. The current results imply that wintertime aerosol pollution in Beijing is likely driven by increased coal combustion and possible secondary formation of other aerosol components such as nitrate, sulfate, and organic carbon coemitted with EC.^{15,29,61,67}

In summary, the sources of elemental carbon (EC) from ambient samples collected in Beijing were investigated based on both radiocarbon (¹⁴C) and organic marker measurements. The results demonstrate that EC is dominated by fossil emissions throughout the year with a mean contribution of $79\% \pm 6\%$. To

further identify and quantify traffic-related emissions and coal combustion contributions to fossil EC, hopanes and picene were also measured. The concentrations of the total identified hopanes are $68.6 \pm 28.7 \text{ ng/m}^3$ and $17.9 \pm 6.5 \text{ ng/m}^3$ in the cold and the warm period, respectively. The seasonal molecular pattern of hopanes indicates that vehicle emissions are the most important fossil source in the warm period and coal combustion emission is increased significantly in the cold season. By combining the ¹⁴C and organic marker's measurements, relative contributions from coal and biomass-burning to the excess of EC between the cold and warm seasons were estimated as 68% and 32%, respectively. Based on published data from source samples, the hopane and home-hopane indexes as well as the picene-to-EC ratios are compared among different kinds of coal types. The comparison shows that the residential bituminite is a dominant coal type used during winter in Beijing.

■ ASSOCIATED CONTENT

● Supporting Information

Relevance of the charring reduction using the Swiss_4S protocol; table showing the fraction of modern (f_M) of EC in PM₁, PM_{2.5}, and PM₁₀ in Switzerland; figures describing the fraction of modern (f_M) of EC in PM₄ (winter, 2011) and PM_{2.5} (winter 2013) in Beijing, thermograms of water-extracted aerosol samples using Swiss_4S, integrated probability distributions of the averaged relative contributions to EC from different sources using the Latin-hypercube sampling (LHS) simulation, and the relative contribution to EC from coal combustion (EC_{coal}) as a function of the selected ((picene/EC)_{coal}). The Supporting Information is available free of charge on the ACS Publications website at DOI: 10.1021/acs.est.5b01944.

■ AUTHOR INFORMATION

Corresponding Author

*Phone: +41 31 631 4308; fax: +41 31 631 43 99; e-mail: dryanlinzhang@gmail.com.

Present Address

[†](P.Z.) Lucerne School of Engineering and Architecture, Bioenergy Research, Lucerne University of Applied Sciences and Arts, 6048 Horw, Switzerland.

Notes

The authors declare no competing financial interest.

■ ACKNOWLEDGMENTS

Y.-L.Z. acknowledges partial support from the Swiss National Science Foundation Fellowship. This work is also partially supported by the KIT Centre for Climate and Environment and the Helmholtz Zentrum München, German Research Center for Environmental Health. R.-r. S. acknowledges the PhD Scholarship from the China Scholarship Council (CSC).

■ REFERENCES

- (1) Pope, C. A., III; Dockery, D. W. Health effects of fine particulate air pollution: Lines that connect. *J. Air Waste Manage. Assoc.* **2006**, *56* (6), 709–742.
- (2) WHO. *Air Quality Guidelines: Global Update 2005: Particulate Matter, Ozone, Nitrogen Dioxide and Sulfur Dioxide*; World Health Organization, 2006.
- (3) Jacobson, M. C.; Hansson, H. C.; Noone, K. J.; Charlson, R. J. Organic atmospheric aerosols: Review and state of the science. *Rev. Geophys.* **2000**, *38* (2), 267–294.
- (4) Petzold, A.; Ogren, J. A.; Fiebig, M.; Laj, P.; Li, S. M.; Baltensperger, U.; Holzer-Popp, T.; Kinne, S.; Pappalardo, G.; Sugimoto, N.; Wehrli,

- C.; Wiedensohler, A.; Zhang, X. Y. Recommendations for reporting "black carbon" measurements. *Atmos. Chem. Phys.* **2013**, *13* (16), 8365–8379.
- (5) Ramanathan, V.; Carmichael, G. Global and regional climate changes due to black carbon. *Nat. Geosci.* **2008**, *1* (4), 221–227.
- (6) Weinhold, B. Global Bang for the Buck Cutting Black Carbon and Methane Benefits Both Health and Climate. *Environ. Health Perspect.* **2012**, *120* (6), A245–A245.
- (7) Shindell, D.; Kuylenstierna, J. C. I.; Vignati, E.; van Dingenen, R.; Amann, M.; Klimont, Z.; Anenberg, S. C.; Müller, N.; Janssens-Maenhout, G.; Raes, F.; Schwartz, J.; Faluvegi, G.; Pozzoli, L.; Kupiainen, K.; Hoglund-Isaksson, L.; Emberson, L.; Streets, D.; Ramanathan, V.; Hicks, K.; Oanh, N. T. K.; Milly, G.; Williams, M.; Demkine, V.; Fowler, D. Simultaneously Mitigating Near-Term Climate Change and Improving Human Health and Food Security. *Science* **2012**, *335* (6065), 183–189.
- (8) Bond, T. C.; Doherty, S. J.; Fahey, D. W.; Forster, P. M.; Berntsen, T.; DeAngelo, B. J.; Flanner, M. G.; Ghan, S.; Karcher, B.; Koch, D.; Kinne, S.; Kondo, Y.; Quinn, P. K.; Sarofim, M. C.; Schultz, M. G.; Schulz, M.; Venkataraman, C.; Zhang, H.; Zhang, S.; Bellouin, N.; Guttikunda, S. K.; Hopke, P. K.; Jacobson, M. Z.; Kaiser, J. W.; Klimont, Z.; Lohmann, U.; Schwarz, J. P.; Shindell, D.; Storelvmo, T.; Warren, S. G.; Zender, C. S. Bounding the role of black carbon in the climate system: A scientific assessment. *J. Geophys. Res.* **2013**, *118* (11), 5380–5552.
- (9) Currie, L. A. Evolution and multidisciplinary frontiers of ¹⁴C aerosol science. *Radiocarbon* **2000**, *42* (1), 115–126.
- (10) Szidat, S. Sources of Asian haze. *Science* **2009**, *323* (5913), 470–471.
- (11) Zotter, P.; Ciobanu, V. G.; Zhang, Y. L.; El-Haddad, I.; Macchia, M.; Daellenbach, K. R.; Salazar, G. A.; Huang, R. J.; Wacker, L.; Hueglin, C.; Piazzalunga, A.; Fermo, P.; Schwikowski, M.; Baltensperger, U.; Szidat, S.; Prévôt, A. S. H. Radiocarbon analysis of elemental and organic carbon in Switzerland during winter-smog episodes from 2008 to 2012 – Part 1: Source apportionment and spatial variability. *Atmos. Chem. Phys.* **2014**, *14* (24), 13551–13570.
- (12) Szidat, S.; Bench, G.; Bernardoni, V.; Calzolari, G.; Czimczik, C. I.; Derendorf, L.; Dusek, U.; Elder, K.; Fedi, M.; Genberg, J.; Gustafsson, O.; Kirillova, E.; Kondo, M.; McNichol, A. P.; Perron, N.; Santos, G. M.; Stenstrom, K.; Swietlicki, E.; Uchida, M.; Vecchi, R.; Wacker, L.; Zhang, Y. L.; Prevot, A. S. H. Intercomparison of ¹⁴C Analysis of Carbonaceous Aerosols: Exercise 2009. *Radiocarbon* **2013**, *55* (3–4), 1496–1509.
- (13) Bernardoni, V.; Calzolari, G.; Chiari, M.; Fedi, M.; Lucarelli, F.; Nava, S.; Piazzalunga, A.; Riccobono, F.; Taccetti, F.; Valli, G.; Vecchi, R. Radiocarbon analysis on organic and elemental carbon in aerosol samples and source apportionment at an urban site in Northern Italy. *J. Aerosol Sci.* **2013**, *56*, 88–99.
- (14) Zhang, Y. L.; Perron, N.; Ciobanu, V. G.; Zotter, P.; Minguillón, M. C.; Wacker, L.; Prévôt, A. S. H.; Baltensperger, U.; Szidat, S. On the isolation of OC and EC and the optimal strategy of radiocarbon-based source apportionment of carbonaceous aerosols. *Atmos. Chem. Phys.* **2012**, *12*, 10841–10856.
- (15) Huang, R. J.; Zhang, Y.; Bozzetti, C.; Ho, K. F.; Cao, J. J.; Han, Y.; Daellenbach, K. R.; Slowik, J. G.; Platt, S. M.; Canonaco, F.; Zotter, P.; Wolf, R.; Pieber, S. M.; Bruns, E. A.; Crippa, M.; Ciarelli, G.; Piazzalunga, A.; Schwikowski, M.; Abbazade, G.; Schnelle-Kreis, J.; Zimmermann, R.; An, Z.; Szidat, S.; Baltensperger, U.; El Haddad, I.; Prevot, A. S. H. High secondary aerosol contribution to particulate pollution during haze events in China. *Nature* **2014**, *514* (7521), 218–22.
- (16) Sun, Y. L.; Zhuang, G. S.; Ying, W.; Han, L. H.; Guo, J. H.; Mo, D.; Zhang, W. J.; Wang, Z. F.; Hao, Z. P. The air-borne particulate pollution in Beijing - concentration, composition, distribution and sources. *Atmos. Environ.* **2004**, *38* (35), 5991–6004.
- (17) Duan, F. K.; He, K. B.; Ma, Y. L.; Yang, F. M.; Yu, X. C.; Cadle, S. H.; Chan, T.; Mulawa, P. A. Concentration and chemical characteristics of PM_{2.5} in Beijing, China: 2001–2002. *Sci. Total Environ.* **2006**, *355* (1–3), 264–275.
- (18) Okuda, T.; Katsuno, M.; Naoi, D.; Nakao, S.; Tanaka, S.; He, K. B.; Ma, Y. L.; Lei, Y.; Jia, Y. T. Trends in hazardous trace metal concentrations in aerosols collected in Beijing, China from 2001 to 2006. *Chemosphere* **2008**, *72* (6), 917–924.
- (19) Yang, F.; He, K.; Ye, B.; Chen, X.; Cha, L.; Cadle, S. H.; Chan, T.; Mulawa, P. A. One-year record of organic and elemental carbon in fine particles in downtown Beijing and Shanghai. *Atmos. Chem. Phys.* **2005**, *5*, 1449–1457.
- (20) Zhang, J. K.; Sun, Y.; Liu, Z. R.; Ji, D. S.; Hu, B.; Liu, Q.; Wang, Y. S. Characterization of submicron aerosols during a month of serious pollution in Beijing, 2013. *Atmos. Chem. Phys.* **2014**, *14* (6), 2887–2903.
- (21) Zheng, M.; Salmon, L. G.; Schauer, J. J.; Zeng, L. M.; Kiang, C. S.; Zhang, Y. H.; Cass, G. R. Seasonal trends in PM_{2.5} source contributions in Beijing, China. *Atmos. Environ.* **2005**, *39* (22), 3967–3976.
- (22) Sun, Y. L.; Jiang, Q.; Wang, Z. F.; Fu, P. Q.; Li, J.; Yang, T.; Yin, Y. Investigation of the sources and evolution processes of severe haze pollution in Beijing in January 2013. *J. Geophys. Res.* **2014**, *119* (7), 4380–4398.
- (23) Zhang, Y. L.; Huang, R. J.; El Haddad, I.; Ho, K. F.; Cao, J. J.; Han, Y.; Zotter, P.; Bozzetti, C.; Daellenbach, K. R.; Canonaco, F.; Slowik, J. G.; Salazar, G.; Schwikowski, M.; Schnelle-Kreis, J.; Abbazade, G.; Zimmermann, R.; Baltensperger, U.; Prévôt, A. S. H.; Szidat, S. Fossil vs. non-fossil sources of fine carbonaceous aerosols in four Chinese cities during the extreme winter haze episode of 2013. *Atmos. Chem. Phys.* **2015**, *15* (3), 1299–1312.
- (24) Sun, Y. L.; Zhang, Q.; Schwab, J. J.; Yang, T.; Ng, N. L.; Demerjian, K. L. Factor analysis of combined organic and inorganic aerosol mass spectra from high resolution aerosol mass spectrometer measurements. *Atmos. Chem. Phys.* **2012**, *12* (18), 8537–8551.
- (25) Cheng, Y.; Engling, G.; He, K. B.; Duan, F. K.; Ma, Y. L.; Du, Z. Y.; Liu, J. M.; Zheng, M.; Weber, R. J. Biomass burning contribution to Beijing aerosol. *Atmos. Chem. Phys.* **2013**, *13* (15), 7765–7781.
- (26) Chen, B.; Du, K.; Wang, Y.; Chen, J. S.; Zhao, J. P.; Wang, K.; Zhang, F. W.; Xu, L. L. Emission and Transport of Carbonaceous Aerosols in Urbanized Coastal Areas in China. *Aerosol Air Qual. Res.* **2012**, *12* (3), 371–378.
- (27) Marple, V. A.; Liu, B. Y. H. Characteristics of laminar jet impactors. *Environ. Sci. Technol.* **1974**, *8* (7), 648–654.
- (28) Gussman, R. A. On the Aerosol Particle Slip Correction Factor. *J. Appl. Meteorol.* **1969**, *8* (6), 999–1001.
- (29) Prassertachato, T.; Podgorski, A.; Luckner, J.; Furuuchi, M.; Gradon, L.; Suvachittanont, S.; Szymanski, W. Sampling and characterization of PM-fractions of ambient particulate matter in Bangkok utilizing a cascade virtual impactor. *Aerosol Air Qual. Res.* **2006**, *6* (1), 67–81.
- (30) Zhang, Y. L.; Zotter, P.; Perron, N.; Prévôt, A. S. H.; Wacker, L.; Szidat, S. Fossil and non-fossil sources of different carbonaceous fractions in fine and coarse particles by radiocarbon measurement. *Radiocarbon* **2013**, *55* (2–3), 1510–1520.
- (31) Zhang, H.; Wang, S.; Hao, J.; Wan, L.; Jiang, J.; Zhang, M.; Mestl, H. E. S.; Alnes, L. W. H.; Aunan, K.; Mellouki, A. W. Chemical and size characterization of particles emitted from the burning of coal and wood in rural households in Guizhou, China. *Atmos. Environ.* **2012**, *51* (0), 94–99.
- (32) Huang, X. F.; Yu, J. Z.; He, L. Y.; Hu, M. Size distribution characteristics of elemental carbon emitted from Chinese vehicles: results of a tunnel study and atmospheric implications. *Environ. Sci. Technol.* **2006**, *40* (17), 5355–60.
- (33) Huang, X. F.; Yu, J. Z. Size distributions of elemental carbon in the atmosphere of a coastal urban area in South China: characteristics, evolution processes, and implications for the mixing state. *Atmos. Chem. Phys.* **2008**, *8* (19), 5843–5853.
- (34) Cavalli, F.; Viana, M.; Yttri, K. E.; Genberg, J.; Putaud, J. P. Toward a standardised thermal-optical protocol for measuring atmospheric organic and elemental carbon: The EUSAAR protocol. *Atmos. Meas. Tech.* **2010**, *3* (1), 79–89.
- (35) Schmid, H.; Laskus, L.; Abraham, H. J.; Baltensperger, U.; Lavanchy, V.; Bizjak, M.; Burba, P.; Cachier, H.; Crow, D.; Chow, J.; Gnauk, T.; Even, A.; ten Brink, H. M.; Giesen, K.-P.; Hitznerberger, R.; Hueglin, C.; Maenhaut, W.; Pio, C.; Carvalho, A.; Putaud, J.-P.; Toom-Sauntry, D.; Puxbaum, H. Results of the "carbon conference"

international aerosol carbon round robin test stage I. *Atmos. Environ.* **2001**, *35* (12), 2111–2121.

(36) Piazzalunga, A.; Bernardoni, V.; Fermo, P.; Valli, G.; Vecchi, R. Technical Note: On the effect of water-soluble compounds removal on EC quantification by TOT analysis in urban aerosol samples. *Atmos. Chem. Phys.* **2011**, *11* (19), 10193–10203.

(37) Synal, H. A.; Stocker, M.; Suter, M. MICADAS: A new compact radiocarbon AMS system. *Nucl. Instrum. Methods Phys. Res., Sect. B* **2007**, *259* (1), 7–13.

(38) Wacker, L.; Fahrni, S. M.; Hajdas, I.; Molnar, M.; Synal, H. A.; Szidat, S.; Zhang, Y. L. A versatile gas interface for routine radiocarbon analysis with a gas ion source. *Nucl. Instrum. Methods Phys. Res., Sect. B* **2013**, *294*, 315–319.

(39) Stuiver, M.; Polach, H. A. Reporting of C-14 data - discussion. *Radiocarbon* **1977**, *19* (3), 355–363.

(40) Wacker, L.; Christl, M.; Synal, H. A. Bats: A new tool for AMS data reduction. *Nucl. Instrum. Methods Phys. Res., Sect. B* **2010**, *268* (7–8), 976–979.

(41) Orasche, J.; Schnelle-Kreis, J.; Abbaszade, G.; Zimmermann, R. Technical Note: In-situ derivatization thermal desorption GC-TOFMS for direct analysis of particle-bound non-polar and polar organic species. *Atmos. Chem. Phys.* **2011**, *11* (17), 8977–8993.

(42) Wang, Q.; Shao, M.; Zhang, Y.; Wei, Y.; Hu, M.; Guo, S. Source apportionment of fine organic aerosols in Beijing. *Atmos. Chem. Phys.* **2009**, *9* (21), 8573–8585.

(43) Yang, F.; Huang, L.; Duan, F.; Zhang, W.; He, K.; Ma, Y.; Brook, J. R.; Tan, J.; Zhao, Q.; Cheng, Y. Carbonaceous species in PM_{2.5} at a pair of rural/urban sites in Beijing, 2005–2008. *Atmos. Chem. Phys.* **2011**, *11* (15), 7893–7903.

(44) Minguillón, M. C.; Perron, N.; Querol, X.; Szidat, S.; Fahrni, S. M.; Alastuey, A.; Jimenez, J. L.; Mohr, C.; Ortega, A. M.; Day, D. A.; Lanz, V. A.; Wacker, L.; Reche, C.; Cusack, M.; Amato, F.; Kiss, G.; Hoffer, A.; Decesari, S.; Moretti, F.; Hillamo, R.; Teinila, K.; Seco, R.; Penuelas, J.; Metzger, A.; Schallhart, S.; Müller, M.; Hansel, A.; Burkhardt, J. F.; Baltensperger, U.; Prevot, A. S. H. Fossil versus contemporary sources of fine elemental and organic carbonaceous particulate matter during the DAURE campaign in Northeast Spain. *Atmos. Chem. Phys.* **2011**, *11* (23), 12067–12084.

(45) Bressi, M.; Sciare, J.; Ghersi, V.; Bonnaire, N.; Nicolas, J. B.; Petit, J. E.; Moukhtar, S.; Rosso, A.; Mihalopoulos, N.; Feron, A. A one-year comprehensive chemical characterisation of fine aerosol (PM_{2.5}) at urban, suburban and rural background sites in the region of Paris (France). *Atmos. Chem. Phys.* **2013**, *13* (15), 7825–7844.

(46) Polidori, A.; Turpin, B. J.; Lim, H. J.; Cabada, J. C.; Subramanian, R.; Pandis, S. N.; Robinson, A. L. Local and regional secondary organic aerosol: Insights from a year of semi-continuous carbon measurements at Pittsburgh. *Aerosol Sci. Technol.* **2006**, *40* (10), 861–872.

(47) Zhang, Y.-L.; Li, J.; Zhang, G.; Zotter, P.; Huang, R.-J.; Tang, J.-H.; Wacker, L.; Prévôt, A. S. H.; Szidat, S. Radiocarbon-based source apportionment of carbonaceous aerosols at a regional background site on Hainan Island, South China. *Environ. Sci. Technol.* **2014**, *48* (5), 2651–2659.

(48) Chen, B.; Andersson, A.; Lee, M.; Kirillova, E. N.; Xiao, Q.; Krusa, M.; Shi, M.; Hu, K.; Lu, Z.; Streets, D. G.; Du, K.; Gustafsson, O. Source forensics of black carbon aerosols from China. *Environ. Sci. Technol.* **2013**, *47* (16), 9102–8.

(49) Liu, J. W.; Li, J.; Zhang, Y. L.; Liu, D.; Ding, P.; Shen, C. D.; Shen, K. J.; He, Q. F.; Ding, X.; Wang, X. M.; Chen, D. H.; Szidat, S.; Zhang, G. Source Apportionment Using Radiocarbon and Organic Tracers for PM_{2.5} Carbonaceous Aerosols in Guangzhou, South China: Contrasting Local- and Regional-Scale Haze Events. *Environ. Sci. Technol.* **2014**, *48* (20), 12002–12011.

(50) Watson, J. G.; Chow, J. C. Source characterization of major emission sources in the Imperial and Mexicali Valleys along the US/Mexico border. *Sci. Total Environ.* **2001**, *276* (1–3), 33–47.

(51) Kaplan, I. R.; Lu, S. T.; Alimi, H. M.; MacMurphey, J. Fingerprinting of high boiling hydrocarbon fuels, asphalts and lubricants. *Environ. Forensics* **2001**, *2* (3), 231–248.

(52) Rogge, W. F.; Hildemann, L. M.; Mazurek, M. A.; Cass, G. R.; Simoneit, B. R. T. Sources of fine organic aerosol 0.8. Boilers burning No. 2 distillate fuel oil. *Environ. Sci. Technol.* **1997**, *31* (10), 2731–2737.

(53) Oros, D. R.; Simoneit, B. R. T. Identification and emission rates of molecular tracers in coal smoke particulate matter. *Fuel* **2000**, *79* (5), 515–536.

(54) Rogge, W. F.; Hildemann, L. M.; Mazurek, M. A.; Cass, G. R.; Simoneit, B. R. T. Sources of Fine Organic Aerosol 0.2. Noncatalyst and Catalyst-Equipped Automobiles and Heavy-Duty Diesel Trucks. *Environ. Sci. Technol.* **1993**, *27* (4), 636–651.

(55) Schnelle-Kreis, J.; Sklorz, M.; Peters, A.; Cyrys, J.; Zimmermann, R. Analysis of particle-associated semi-volatile aromatic and aliphatic hydrocarbons in urban particulate matter on a daily basis. *Atmos. Environ.* **2005**, *39* (40), 7702–7714.

(56) Schnelle-Kreis, J.; Sklorz, M.; Orasche, J.; Stolzel, M.; Peters, A.; Zimmermann, R. Semi volatile organic compounds in ambient PM_{2.5}: Seasonal trends and daily resolved source contributions. *Environ. Sci. Technol.* **2007**, *41* (11), 3821–3828.

(57) El-Gayar, M. S.; Abdelfattah, A. E.; Barakat, A. O. Maturity-dependent geochemical markers of crude petroleum from Egypt. *Pet. Sci. Technol.* **2002**, *20* (9–10), 1057–1070.

(58) Czechowski, F.; Stolarski, M.; Simoneit, B. R. T. Supercritical fluid extracts from brown coal lithotypes and their group components - molecular composition of non-polar compounds. *Fuel* **2002**, *81* (15), 1933–1944.

(59) Fraser, M. P.; Cass, G. R.; Simoneit, B. R. T. Gas-phase and particle-phase organic compounds emitted from motor vehicle traffic in a Los Angeles roadway tunnel. *Environ. Sci. Technol.* **1998**, *32* (14), 2051–2060.

(60) Robinson, A. L.; Subramanian, R.; Donahue, N. M.; Bernardo-Bricker, A.; Rogge, W. F. Source apportionment of molecular markers and organic aerosols-1. Polycyclic aromatic hydrocarbons and methodology for data visualization. *Environ. Sci. Technol.* **2006**, *40* (24), 7803–7810.

(61) Zhang, Y. X.; Schauer, J. J.; Zhang, Y. H.; Zeng, L. M.; Wei, Y. J.; Liu, Y.; Shao, M. Characteristics of particulate carbon emissions from real-world Chinese coal combustion. *Environ. Sci. Technol.* **2008**, *42* (14), 5068–5073.

(62) Chen, Y. J.; Sheng, G. Y.; Bi, X. H.; Feng, Y. L.; Mai, B. X.; Fu, J. M. Emission factors for carbonaceous particles and polycyclic aromatic hydrocarbons from residential coal combustion in China. *Environ. Sci. Technol.* **2005**, *39* (6), 1861–1867.

(63) Gelencsér, A.; May, B.; Simpson, D.; Sánchez-Ochoa, A.; Kasper-Giebl, A.; Puxbaum, H.; Caseiro, A.; Pio, C.; Legrand, M. Source apportionment of PM_{2.5} organic aerosol over Europe: Primary/secondary, natural/anthropogenic, and fossil/biogenic origin. *J. Geophys. Res.* **2007**, *112* (D23), D23S04.

(64) Szidat, S.; Ruff, M.; Perron, N.; Wacker, L.; Synal, H.-A.; Hallquist, M.; Shannigrahi, A. S.; Yttri, K. E.; Dye, C.; Simpson, D. Fossil and non-fossil sources of organic carbon (OC) and elemental carbon (EC) in Goeteborg, Sweden. *Atmos. Chem. Phys.* **2009**, *9*, 1521–1535.

(65) Yttri, K. E.; Simpson, D.; Stenström, K.; Puxbaum, H.; Svendby, T. Source apportionment of the carbonaceous aerosol in Norway-quantitative estimates based on ¹⁴C, thermal-optical and organic tracer analysis. *Atmos. Chem. Phys.* **2011**, *11* (17), 9375–9394.

(66) Genberg, J.; Hyder, M.; Stenström, K.; Bergström, R.; Simpson, D.; Fors, E.; Jönsson, J. Å.; Swietlicki, E. Source apportionment of carbonaceous aerosol in southern Sweden. *Atmos. Chem. Phys.* **2011**, *11* (22), 11387–11400.

(67) Lu, Z.; Zhang, Q.; Streets, D. G. Sulfur dioxide and primary carbonaceous aerosol emissions in China and India, 1996–2010. *Atmos. Chem. Phys.* **2011**, *11* (18), 9839–9864.